Research article

Sensorless Based Haptic Feedback Integration In Robot-assisted Pedicle Screw Insertion For Lumbar Spine Surgery: A preliminary cadaveric study

Sakol Nakdhamabhorn [a], Branesh M. Pillai [a], Areesak Chotivichit [b], Jackrit Suthakorn [a],*

[a] *Department of Biomedical Engineering, Center for Biomedical and Robotics Technology (BART LAB), Faculty of Engineering, Mahidol University, Nakhon Pathom 73170, Thailand*
[b] *Department of Orthopedic Surgery, Faculty of Medicine Siriraj Hospital, Mahidol University, Thailand*

ARTICLE INFO

ABSTRACT

Pedicle screw fixation is an essential surgical technique for addressing various spinal pathologies, including degenerative diseases, trauma, tumors, neoplasms, and infections. Despite its efficacy, the procedure poses significant challenges, notably the limited visibility of spinal anatomical landmarks and the consequent reliance on surgeon's hand-eye coordination. These challenges often result in inaccuracies and high radiation exposure due to the frequent use of fluoroscopy X-ray guidance. Addressing these concerns, this study introduces a novel approach to pedicle screw insertion by utilizing a robot-assisted system that incorporates sensorless based haptics incorporated 5-DOF surgical manipulation. This innovative system aims to minimize radiation exposure and reduce operating time while improving the surgeon's hand posture capabilities. The developed prototype, expected to be implemented using bilateral control, was tested through preliminary cadaveric experiments focused on the insertion of both percutaneous and open pedicle screws at the L4-L5 level of the lumbar spine. Validation of the Sensorless Haptic Feedback feature was an integral part of this study, aiming to enhance precision and safety. The results, confirmed by fluoroscopic x-ray images, demonstrated the successful placement of two percutaneous and two open pedicle screws, with average position and torque errors of 0.011 radians and 0.054 Nm for percutaneous screws, and 0.0116 radians and 0.0057 Nm for open screws, respectively. These findings underscore the potential of the sensorless haptic feedback in a robot-assisted pedicle screw insertion system to significantly reduce radiation exposure and improve surgical outcomes, marking a significant advancement in spinal surgery technology.

1. Introduction

Pedicle screw fixation is a cornerstone technique in spinal surgery, widely used to treat a variety of spinal pathologies, including degenerative disc disease, spinal trauma, tumors, and infections [1,2]. This surgical method involves the placement of screws into the pedicle of the vertebral arch to stabilize and support the spine [3]. While pedicle screw fixation has proven to be effective, its success heavily depends on the precise placement of the screws, which can be challenging due to the complex anatomy of the spine and the limited visibility of key anatomical landmarks during surgery [4]. The traditional approach to pedicle screw insertion often requires the surgeon to rely extensively on hand-eye coordination and fluoroscopic guidance to navigate these challenges [5,6]. However, this reliance on fluoroscopy exposes both the patient and the surgical team to potentially harmful radiation.

Moreover, the manual placement of pedicle screws carries inherent risks of inaccuracies, which can lead to complications such as nerve damage, screw misplacement, or suboptimal stabilization of the spine [7–11]. Such inaccuracies not only jeopardize patient outcomes but also increase the likelihood of revision surgeries, which are burdensome for both patients and healthcare systems [12–14]. Fig. 1 shows a skillful surgeon performing percutaneous insertion of the pedicle screw at the Faculty of Medicine Siriraj Hospital, Mahidol University.

Current practices often necessitate the use of multiple fluoroscopic images to determine screw placement trajectories, which may increase x-ray exposure for both surgeons and patients [15–17]. Radiation exposure levels to the chief surgeon during a single procedure are measured at 1.7 μSv for the entire body, 204.7 μSv for extremities, and 30.5 μSv for the lens, as documented in source [18]. According to safety standards set by the International Commission on Radiological

Protection (ICRP) [19,20] and the European Directive (2013/59/Euratom) [21], the maximum allowable average exposure is limited to 20 mSv annually, effectively restricting a surgeon to a maximum of 655 procedures per year. The mention of 655 annual fusions in the study indicates the theoretical maximum number of procedures a surgeon could undertake under current radiation safety guidelines from the ICRP and the European Directive. This figure does not suggest that surgeons commonly perform this number of surgeries; rather, it specifies the potential upper limit of procedures allowed under the current radiation safety regulations, assuming continuous operation at the allowed annual radiation exposure limit. This restriction leads to a shortage of available surgeons, subsequently prolonging wait times for necessary surgeries. Furthermore, inaccuracies in screw placement can compromise neurovascular integrity and spinal stability. In response to these challenges, several commercially available robotic systems are designed to aid in pedicle screw insertion [22].

Spine Assist, developed by Mazor Robotics, represents an early foray into robot-assisted spine surgery [23]. This system features a miniature parallel robotic manipulator that attaches directly to the patient's spine. Surgical planning and navigation are facilitated through the use of CT scans and fiducial markers. An upgraded version, known as Renaissance, retains the core technology but introduces enhancements to the planning software and user interface [24–26]. The most recent iteration from Mazor Robotics, MazorX, includes a 6-DOF manipulator equipped with advanced planning and navigation software [27,28]. Additionally, Medtech in Montpellier, France, has developed the ROSA Spine, which comprises a 6-DOF articular robot manipulator on a workstation with a compact touchscreen [29,30]. Another significant development, Excelsius GPS by Globus Medical based in Audubon, PA, features a robotic manipulator positioned on a base station adjacent to the patient's operation bed, integrating a camera tracking system with preoperative CT scans to guide the robot's end-effector trajectory [31,32]. Despite these innovations, commercial robotic systems present challenges, including a complex and costly nature which necessitates a steep learning curve for surgeons and requires specialized tools for operation and maintenance [33]. While navigation-based methods like the use of O-arm or 3D C-arm have become popular for their ability to limit radiation exposure with just a single preoperative image, they still expose patients to a significant initial radiation dose. In response to these challenges, the development of robotic-assisted surgical systems has emerged as a significant innovation, aiming to enhance the precision and safety of pedicle screw fixation. These systems utilize advanced robotics combined with real-time imaging to aid surgeons in the accurate placement of screws. Despite these advancements, current robotic systems often still require some level of fluoroscopic guidance, which continues to expose patients to radiation.

Addressing this critical issue, this study introduces an approach that integrates sensorless haptic feedback within a robotic-assisted surgical system. This system is designed to reduce dependence on fluoroscopic imaging, thereby minimizing radiation exposure while aiming to maintain, if not enhance, the accuracy and efficiency of the surgical procedure. In contrast, the proposed sensorless-based haptic feedback in robot-assisted pedicle screw insertion eliminates the need for intraoperative fluoroscopy [34]. The design of this system provides real-time feedback without additional imaging following the initial setup, detecting physical boundaries and anatomical structures, which may significantly reduce subsequent radiation exposure. The primary advancement of this study, the integration of sensorless haptic feedback, addresses issues of limited visibility and predictability of robotic actions during surgery by providing tactile feedback through the master control. This allows surgeons to 'feel' the placement of screws, significantly reducing the need for constant visual monitoring of the slave arm. Additionally, the use of a bilateral control system ensures synchronized and safe movement of both the master and slave arms, enhancing coordination and reducing the cognitive load on the surgeon.

The robotic arm developed in this study integrates sensorless haptic feedback and a 5-DOF surgical manipulator, designed to enhance the precision of screw placement without the need for continuous fluoroscopic guidance, significantly reducing radiation exposure and aligning with medical directives aimed at minimizing risks associated with ionizing radiation [35]. This system automates some aspects of the screw insertion process, improving placement accuracy and potentially shortening surgery duration. Such reductions are beneficial not only from a clinical efficiency standpoint but also in minimizing the patient's exposure to anesthesia and the risks of prolonged surgical procedures. Moreover, the sensorless based master-slave setup further refines screw placement precision, with cadaveric study feedback suggesting that the system's torque and positional accuracy are comparable to, if not better than, traditional and other robotic-assisted techniques [36]. This high level of precision is critical, particularly in complex cases, where even minor deviations can result in significant complications. Preliminary results from our study demonstrated successful placement of pedicle screws with minimal position and torque errors, suggesting that despite the complexities of using dual arms, the system's performance in terms of precision and safety is promising. Compared to traditional methods that rely solely on image guidance, our robotic system significantly
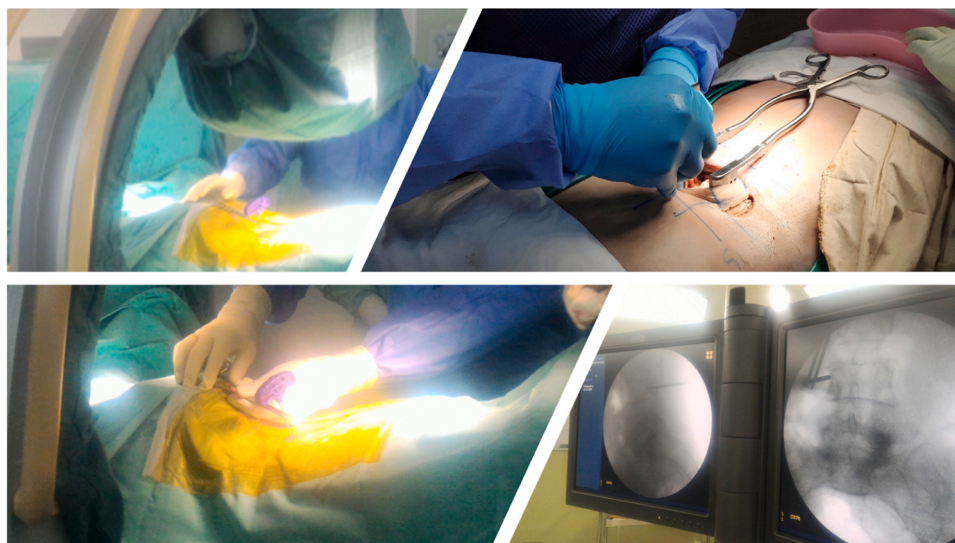

Fig. 1. The percutaneous and open pedicle screw insertion procedure at the Faculty of Medicine Siriraj Hospital, Mahidol University.

reduces radiation exposure and operational time, which are critical in spinal surgery [37–39].

The preliminary cadaveric experiments of this study tested the prototype's effectiveness in controlled settings, focusing on the insertion of both percutaneous and open pedicle screws. These experiments evaluated the accuracy of screw placement based on minimal position and torque errors. A key aspect of the study was validating the Sensorless Haptic Feedback feature, which provides real-time feedback to the surgeon, potentially reducing reliance on intraoperative fluoroscopy and thereby minimizing radiation risks to both the surgical team and patients. Additionally, the study suggests that the system could decrease operating times by offering immediate feedback, thus speeding up decision-making processes that typically rely on fluoroscopic or navigational screen validation. As a preliminary research effort, this study marks the beginning of a larger investigation needed to confirm these findings through more extensive clinical trials, assessing advantages such as outcomes, cost-effectiveness, learning curves, and integration into existing surgical workflows.

2. Materials and methods

Cadaveric based experiments were conducted, and the study was conducted in accordance with the Declaration of Helsinki and approved by the Institutional Review Board of the Mahidol University, SIRB Protocol No: 568/2563 for studies involving humans. Informed consent was obtained from the family members/ surrogate of all cadavers involved in the study. Family members/ surrogate also provided written informed consent for the publication of the data. In this study authors proposes three specific hypotheses: 1) the system can reduce the need for intraoperative fluoroscopy, thereby decreasing radiation exposure for both cadaver and the surgical team; 2) it can improve the accuracy of pedicle screw placement over traditional methods, as evidenced by lower position and torque errors; and 3) it can decrease operating time by providing real-time feedback that aids surgeons in making quicker decisions. These hypotheses were tested through preliminary cadaveric experiments that involved the insertion of both percutaneous and open pedicle screws at the L4-L5 level using a master slave based 5-DOF surgical manipulator. The pedicle screw insertion for the lumbar spine was carried out on a normal adult cadaver without spine abnormalities or trauma. The cadaver source study was conducted at the Bangkok Biomaterial Center, a part of Siriraj Hospital, Mahidol University. The surgical procedure was performed on the L4-L5 lumbar spinal level of the cadaver, with the percutaneous approach being done on the right side of the vertebrae and the open procedure being performed on the left side of the vertebrae.

2.1. Experimental protocol and methodology

The experimental procedure using this system includes several key steps. Initially, preoperative planning and setup involve imaging the cadaver's spine with standard preoperative techniques to map out the surgical site, which serves as the initial dataset for the system's guidance protocol. Prior to surgery, the system undergoes calibration and initialization, setting up the robot's arms and the sensorless haptic feedback mechanism to align with the cadaver's anatomical data from the preoperative scans. During the surgery, a standard surgical approach to the lumbar spine is performed, typically involving a midline incision followed by the dissection of soft tissues to expose the bony landmarks of the L4-L5 vertebrae. Once the surgeon begins the pedicle screw insertion, the sensorless haptic feedback system is activated, providing real-time tactile feedback on the positioning and force being applied, thereby enhancing the surgeon's perception of the surgical environment without the need for direct visual or radiographic confirmation.

Pedicle screws are inserted using the robot-assisted system, either percutaneously or through an open approach at the L4-L5 level, with the robot guiding the placement based on preoperative planning and the

sensorless haptic feedback assisting in adjusting the trajectory and depth to avoid breaches. After placement, the positions of the screws are confirmed with fluoroscopic x-ray images, and any necessary adjustments are made, aiming to minimize their number and frequency by relying on the accuracy of the haptic feedback. Following confirmation that the screws are correctly positioned; the surgical site is closed in layers according to standard procedures. Postoperative imaging is conducted to validate the success of the surgical procedure and the accuracy of the screw placement. This detailed description highlights the integration of sensorless haptic feedback technology into traditional surgical workflows, addressing challenges such as limited visibility and high reliance on fluoroscopy. As this is a preliminary study, the focus was on demonstrating the feasibility and potential enhancements in precision and safety offered by the haptic feedback in robot-assisted pedicle screw insertion.

2.2. System overview

The overall system of this study involves a dual-station setup comprising a surgeon workstation and a cadaveric station. The surgeon's workstation is equipped with a master robot manipulator that includes a touchscreen display interface, a high-resolution video display, and an X-ray fluoroscopy image display. Additionally, an X-ray radiation shield screen is installed at this station to protect against X-ray exposure during procedures. The cadaveric station features a slave robot manipulator mounted on a mobile platform positioned adjacent to the operation bed. This manipulator replicates the movements of the surgeon's hand, controlled from the master manipulator at the surgeon's workstation. The master manipulator is integral to the system, providing intuitive control over the surgical instruments and translating the surgeon's hand movements into precise actions by the robotic arm. This setup utilizes a bilateral control system that accurately reflects even the slightest adjustments made by the surgeon, enhancing the control over the procedure while minimizing the risk of errors and reducing the reliance on fluoroscopic guidance. Furthermore, the ergonomic design of this system supports a natural hand posture for the surgeon, reducing fatigue and improving overall comfort during the delicate task of pedicle screw insertion. This approach is illustrated in Fig. 2 of the study.

2.3. Robot manipulator design and prototype

To ensure effective pedicle screw placement, it is crucial to analyze the workspace required for the procedure, ensuring that the robot manipulator can access all necessary positions and orientations. This analysis involves determining the concise operational workspace based on the anatomical dimensions of the vertebrae. According to Alon Wolf et al. [40], these dimensions were collected from 55 patients across various age groups and encompass five levels of spinal columns (L1-L5), measured using CT scans. This data helps establish the required volume for the robot's workspace specifically tailored for percutaneous pedicle screw insertion. Notably, the average angle for pedicle entry is 13.7 degrees, reaching up to 22.5 degrees, with a comprehensive angle covering both sides of the pedicle at 45 degrees. The average workspace dimensions for the lumbar spine were found to be 93x28x77 mm, a finding similarly observed by Busscher et al. [41] using the CT scan method. In traditional pedicle screw insertion techniques, a surgeon begins by placing a pedicle needle at the entry point, subsequently adjusting its orientation to navigate into the pedicle body. This orientation adjustment is managed by a remote center of motion (RCM) mechanism [42], which precisely controls the needle's lateral and angular movements. The RCM serves as the pivotal point for screw insertion, guiding the pedicle needle from the entry point through the pedicle into the vertebral body. In this robotic system, the RCM's movements are tightly regulated by the software control system, which utilizes a robot kinematics algorithm to ensure precise manipulation and positioning.
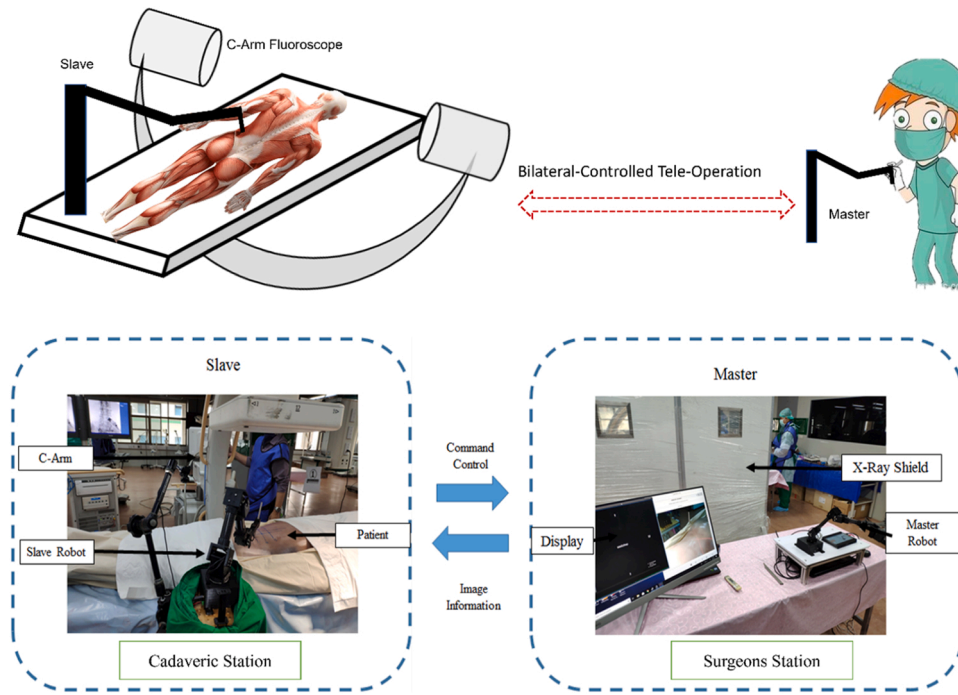
Fig. 2. The system overview of robot-assisted pedicle screw insertion.

The design of the robot manipulator is centered on an assistive concept, where the robot works in cooperation with a surgeon to simplify the system's learning curve. Preliminary findings suggest the robot-assisted system may enhance the surgeon's steady hand ability, dexterity, and precision. While designed to improve radiation safety, definitive claims require further validation through comprehensive clinical trials. The structure of the robot manipulator is X-ray transparent, allowing it to function under fluoroscopy. The system employs a bilateral control setup, featuring a master and a slave manipulator that facilitate the teleoperation procedure. The dimensions of the joints and links of the robot manipulator are tailored to the specific requirements of the pedicle screw insertion workspace and the movements of the surgical tool during operation. Consequently, the robot manipulator is engineered as a 5 DOF serial manipulator, consisting of five actuators and three links, as depicted in Fig. 3.

As illustrated in Fig. 2, the developed robotic system consists of two identical 5 DOF serial manipulators, designed to function as master and slave devices for teleoperation. Both the master and slave manipulators share the same dimensions. While sterilization of the master manipulator at the surgeon's workstation presents minimal concerns, the slave manipulator, which directly interacts with the cadaver, demands rigorous sterilization. To address this, a detachable end-effector link, made from polyacetals (POM), known for their X-ray transparency and suitability for sterilization by dry heating, is attached to the last joint of the slave manipulator. This end-effector holds a stainless-steel hollow tube, serving as a pedicle guidance tool. The tool features an 8 mm diameter, accommodating a smaller diameter guidance tube that adjusts the size to fit different standard pedicle drill bits, as shown in Fig. 3. The actuators of the robot manipulator provide real-time feedback on position, velocity, and current, and are primarily controlled through PID position and velocity control systems. This real-time feedback is integral to the controlled algorithm, enabling effective bilateral operations [43]. Additionally, the software control system and user interface are managed via a Robot Operation System (ROS) platform, enhancing the
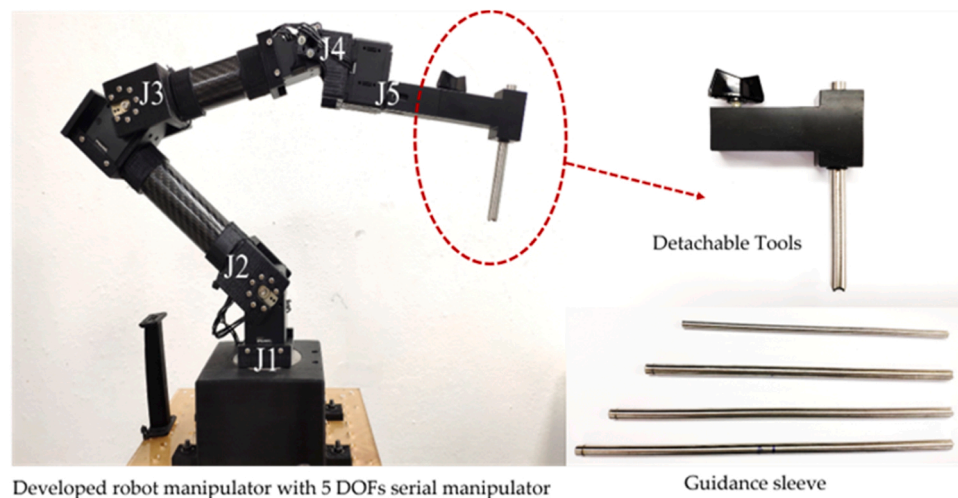

Fig. 3. The Developed robot manipulator with 5 DOF serial manipulator.

functionality and user interaction with the robotic system.

The kinematic relationships and joint coordinate configurations of the developed robot manipulator are detailed in Fig. 4. The setup includes seven joint coordinates which define the operational dynamics of the manipulator concerning its fixed and movable axes. The kinematic relationships of these joint coordinates are illustrated in Fig. 4. The manipulator's base is established as a fixed reference coordinate system. The first frame coordinate operates as a revolute joint, rotating around the Z-axis. Frames 2, 3, and 4 are structured as revolute joints that rotate about the X-axis, and the fifth frame coordinate is a revolute joint rotating around the Y-axis. The tip of the guidance tool, marked as the end-effector coordinate *(ee)*, is defined as a fixed coordinate at the end of the effector. The system utilizes Euler angles to describe a sequence or composition of rotations, providing a clear depiction of the spatial orientation and movement. Typically, 3D rotation matrices are employed to represent the motion across the three rotational axes roll, pitch, and yaw. The matrix representations for these rotations are outlined in Eqs. 1, 2, and 3, respectively, detailing how each rotation impacts the manipulator's positioning and alignment.

$$R_x(\varphi) = \begin{bmatrix} \cos(\varphi) & -\sin(\varphi) & 0 \\ \sin(\varphi) & \cos(\varphi) & 0 \\ 0 & 0 & 1 \end{bmatrix} \tag{1}$$

$$R_y(\emptyset) = \begin{bmatrix} \cos(\emptyset) & -\sin(\emptyset) & 0 \\ \sin(\emptyset) & \cos(\emptyset) & 0 \\ 0 & 0 & 1 \end{bmatrix} \tag{2}$$

$$R_z(\theta) = \begin{bmatrix} \cos(\theta) & -\sin(\theta) & 0 \\ \sin(\theta) & \cos(\theta) & 0 \\ 0 & 0 & 1 \end{bmatrix} \tag{3}$$
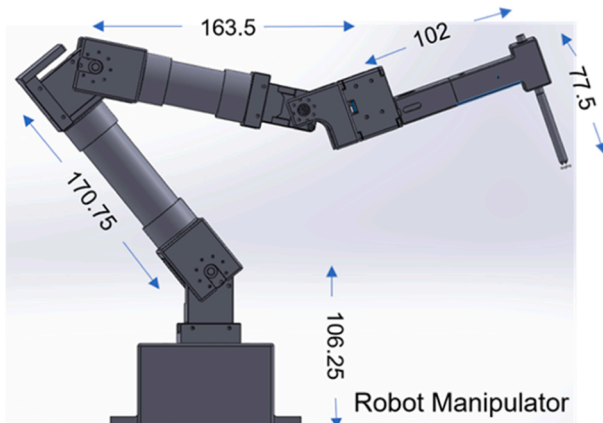
Using (4), the transformation matrix between two consecutive frames is typically represented. The link twist, denoted as $\alpha(i-1)$, is the angle from $z(i-1)$ to $z(i)$, measured around $x(i-1)$ according to the right-hand rule. The link length, $a(i-1)$, is defined as the distance between $z(i-1)$ and $z(i)$ along the $x(i-1)$ direction. The link offset, d_i, represents the displacement between $x(i-1)$ and $x(i)$ along the $z(i)$ axis.

$$H_i^{i-1} = \begin{bmatrix} c\theta_i & -s\theta_i & 0 & \alpha_{i-1} \\ s\theta_i c\alpha_{i-1} & c\theta_i c\alpha_{i-1} & -s\alpha_{i-1} & -s\alpha_{i-1}d_i \\ s\theta_i s\alpha_{i-1} & c\theta_i s\alpha_{i-1} & c\alpha_{i-1} & c\alpha_{i-1}d_i \\ 0 & 0 & 0 & 1 \end{bmatrix} \tag{4}$$

Where, $c\theta_i = \cos\theta_i$; $s\theta_i = \sin\theta_i$; $c\alpha_{i-1} = \cos\alpha_{i-1}$; $s\alpha_{i-1} = \sin\alpha_{i-1}$

$$H = \begin{bmatrix} R_{3\times3} & T_{3\times1} \\ 0 & 1 \end{bmatrix} \tag{5}$$

The kinematic relationship between each frame coordinate is determined using homogeneous transformation matrices, as outlined in (6), which modifies (4) and (5) [44–47].

Definitions include:

H: homogeneous transformation matrix.

R: 3 × 3 rotation matrices.

T: 3 × 1 position vector.

Thus, the transformation from a base frame coordinate to an end-effector frame coordinate is computed using (4), through a series of kinematic transformations as demonstrated in (6).

$$_{Base}^{ee}H = {}_{Base}^{1}H * {}_1^2H * {}_2^3H * 34H * 45H * 5eeH \tag{6}$$

The series of kinematic transformations establishes the reachability of the end effector guidance tooltip by analyzing the joint constraints, thus defining the robot manipulator's reachable workspace. Forward kinematic analysis was conducted using the Robot Operating System (ROS) [48]. The kinematic configuration of the robot manipulator is described using the Unified Robot Description Format (URDF) within ROS. The URDF includes kinematic and basic dynamic descriptions, along with a 3D model of the manipulator, which is displayed on the graphic user interface at the surgeon's workstation. Fig. 5 illustrates the manipulator's reachable workspace as determined by forward kinematic analysis, covering dimensions of *872.5 × 436.25 × 654.25 mm.* The areas reachable by the manipulator are marked in blue, while regions beyond its capability are highlighted in red. An inverse kinematics solver determines the joint angles required to achieve a specific guidance tooltip position and orientation [49]. Inverse kinematics are calculated using closed-form solutions coupled with a search-based approach [45]. Initially, the chain of kinematic transformations identifies all possible joint variable constraints as defined by the transformation in (6). The inverse kinematics solver then seeks the simplest and most straightforward solution. This constraint is refined by sequentially adjusting the kinematic chain frame-by-frame. To address the 6 degrees of freedom (translation and rotation), the algorithm separately resolves the 3 DOFs for translation and 3 DOFs for rotation to produce a closed-form solution. To determine the last three joint angles (θ_4, θ_5, and θ_6), the inverse orientation problem was solved. Individual DH transformations were used to obtain the final transformations. Consequently, the resulting rotation was determined as illustrated in (7). According to (8), the product of the individual rotations between the links equals the total roll, pitch, and yaw (RPY) rotation between the base link and gripper link.

$$_6^0R = {}_1^0R * {}_2^1R * {}_3^2R * 43R * 54R * 65R \tag{7}$$

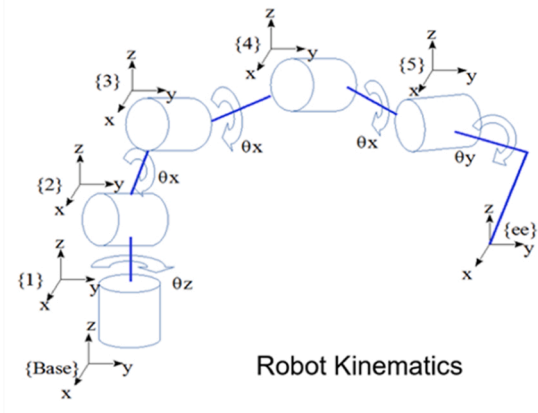$$R_{ee} = {}_6^0R \tag{8}$$

Fig. 4. The kinematic relationship of the developed robot manipulator.
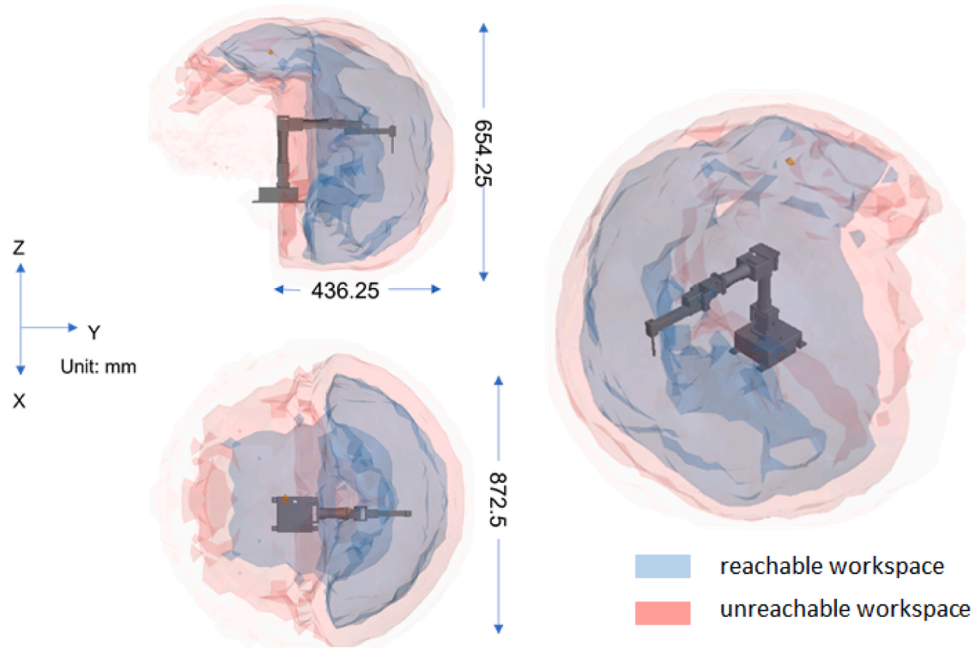
Fig. 5. The reachable workspace of a manipulator.

2.4. Robot control: bilateral control system

Fig. 6 illustrates the bilateral robotic manipulator system, which is designed to convey force sensations through an action-reaction relationship, allowing for intuitive control and interaction. The system comprises two stations: the surgeon station, equipped with the master robotic manipulator, and the cadaver station, where the slave manipulator is located [50]. Through the master manipulator, the surgeon can control the slave, sending motion commands and receiving force feedback, thereby facilitating a dynamic exchange between the two [51–53]. Innovatively, the system employs a sensorless torque sensor rather than traditional force sensors. This sensor leverages both a disturbance observer (DOB) and a reaction torque observer (RTOB) to monitor and adjust the torques within the system [52]. The DOB estimates and compensates for external disturbances to enhance performance, while the RTOB focuses on measuring reaction torques to maintain system stability and control [54,55]. These observers work in tandem to estimate the interaction forces between the master and slave manipulators without direct force measurement, thus improving the system's accuracy and responsiveness in force control [56,57]. The RTOB, essentially a modified DOB, estimates real-time external torque reactions from the slave manipulator, using the system's internal disturbances to calculate reaction torque [58]. This advanced approach allows for a precise control environment in robotic operations.

3. Experiment and results

The experimental configuration employed in this study is a standard setup for pedicle screw insertion procedures. The slave manipulator was positioned near the operating bed at the lumbar location of the cadaver. To establish the surgeon's workstation, an X-ray shield screen was mounted. The workstation included a display monitor and a master manipulator. To perform a comparative analysis, two distinct types of experiments were conducted: percutaneous and open pedicle screw insertion. The surgical procedure was carried out on the L4-L5 lumbar spinal level of the cadaver, with the percutaneous approach being performed on the right side of the vertebrae and the open procedure being performed on the left side of the vertebrae. The experimental setup is illustrated in Fig. 7.
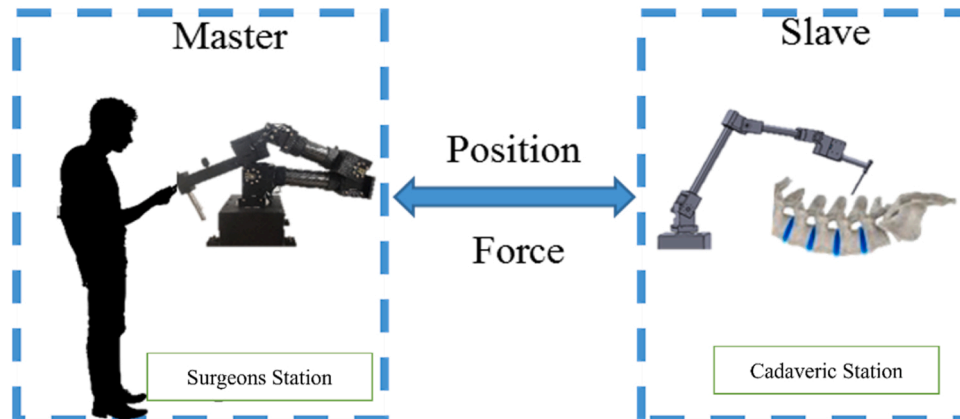

Fig. 6. The robot control: bilateral control system.

Fig. 7. The robot assisted percutaneous pedicle screw insertion: experiment setup.

Fig. 8. Robot-assisted pedicle screw Insertion (a) The slave manipulator placed to the entry point of pedicel (b) Surgeon controlled the master manipulator at workstation (c) The real-time fluoroscopic x-ray and patient video image. (d) The small, guided sleeve inserted into end-effector of manipulator (e) The percutaneous pin traversed a guided sleeve and penetrated the pedicle (f) The K-wire inserted into the pedicle.

3.1. Cadaveric experiment: robot- assisted percutaneous pedicle screw insertion

In this experiment depicted in Fig. 8, a surgeon performs conventional percutaneous pedicle screw insertion using a robot-assisted system to enhance precision and control. The procedure begins with the surgeon manually positioning the robot's slave manipulator, which is equipped with a guidance tool. The tip of this tool must be accurately placed at the intended entry point on the pedicle a critical step for successful screw insertion. The surgeon does this passively without activating the robotic movements. Following the initial setup, the surgeon transitions to a separate workstation to remotely control the slave manipulator through teleoperation. This allows the surgeon to conduct the procedure from a distance, reducing radiation exposure typically associated with direct surgical operations. At the workstation, real-time imaging tools such as fluoroscopic and video feeds are utilized, displayed on a monitor to verify the positioning of the tool tip and refine the trajectory for screw insertion. This real-time imaging provides a dynamic view of the operational field, enhancing the surgeon's ability to make necessary adjustments without compromising sterility or exposure. The surgeon then manipulates the guidance tool tip to precisely target the intended location and direction for the pedicle screw insertion, adjusting the tool tip to align with specific anatomical features and the planned trajectory. The final positioning of the guidance tool is achieved by the system mirroring the surgeon's hand movements at the workstation, translating the surgeon's manual dexterity into robotic motion and combining human skill with robotic precision. The surgeon controlled the slave manipulator until the guidance tool was accurately positioned along the correct trajectory for pedicle screw insertion. A percutaneous pin was then inserted into the guiding tube, and its position was verified using a lateral plane fluoroscopic image to ensure it remained lateral to the medial pedicle wall. After confirming the position of the percutaneous pin, the pin was removed from the guidance tube, and a K-wire guide was inserted through the pedicle of the vertebra using the guidance tube. Following the insertion of the K-wire, the slave manipulator was detached from the cadaver, leaving the K-wire in place. To validate the results of the percutaneous pedicle screw insertion, fluoroscopic images were taken. The pedicle screws were successfully implanted into the cadaver's L4 and L5 lumbar spines as illustrated in Fig. 9.

Fig. 10 illustrates the efficacy of the sensorless based bilaterally controlled robotic system used for percutaneous pedicle screw insertion, providing a detailed visual representation of the position and torque responses between the master and slave manipulators across five joints. The results demonstrate the precision with which the slave manipulator's joint movements mirror those of the master manipulator, with minimal average joint position errors of 0.008, 0.009, 0.012, 0.015, and 0.011 radians for joints 1 through 5, respectively, indicating a high degree of accuracy essential for the delicate task of pedicle screw insertion. Additionally, the torque interaction errors between the manipulators were also found to be small, with average torque response

errors recorded at 0.008, 0.009, 0.012, 0.014, and 0.011 Nm for joints 1 to 5, respectively. This low error rate in torque response ensures that the force applied by the surgeon is effectively translated by the robotic system, maintaining the necessary precision for surgical tasks. Overall, these results substantiate the effectiveness of the sensorless bilaterally controlled system, showcasing its potential to enhance the accuracy and safety of robotic-assisted spinal surgeries. The graphical data from Fig. 10, broken down into subfigures **(a-e)** for position responses and **(f-j)** for torque errors, provides a clear and quantitative demonstration of the system's performance across multiple operational parameters.

3.2. Open pedicle screw insertion: robot- assisted percutaneous pedicle screw insertion

In this phase, the process of open pedicle screw insertion utilizing robot-assisted technology was methodically explored and documented. This procedure involves several critical steps, each carefully controlled and monitored to ensure precision and safety. Initially, the surgeon positions the slave manipulator at the entry point of the pedicle. This specific location is strategically chosen based on anatomical landmarks: it is where the axial plane, passing through the middle of the transverse process, intersects with the sagittal plane that runs through the superior facet. The accuracy of this positioning is crucial as it sets the foundation for the entire procedure. These critical alignment details are visually represented in Figs. 11**(a)** and 11**(b)**. Operating remotely from a workstation that is situated outside the direct X-ray radiation area ensures the surgeon's safety from prolonged radiation exposure, which is a significant concern in traditional surgical settings. From this station, the surgeon proceeds with the next phase of the procedure, employing fluoroscopic imaging to validate the placement and trajectory of the pedicle screw. This imaging step is vital as it confirms that the manipulator and subsequently the screw are correctly aligned with the anatomical target.

Upon validating the trajectory using the captured fluoroscopic image, the surgeon uses the master manipulator to adjust the slave manipulator remotely. This adjustment is crucial to align the guidance tool with the verified trajectory for screw insertion, detailed in Fig. 11 (c). Following trajectory alignment, a smaller guidance tube is introduced into the guidance tool to narrow its diameter, matching that of the drill bit needed for the pedicle screw insertion. This adaptation is necessary for the precise and safe insertion of the drill into the pedicle cortex. The final drilling is performed through the guidance tool using a high-speed drill, where the surgeon meticulously drills the pedicle screw into the pedicle cortex, a step depicted in Fig. 11(d). The entire procedure culminates with a complete open pedicle screw fixation, as presented in Fig. 12 (a), demonstrating the successful stabilization of the spine segment using the robot-assisted system. The completion and success of the screw placement are subsequently verified through additional fluoroscopic imaging, shown in Fig. 12 (b). This imaging serves as a confirmatory step to ensure that the screw is correctly positioned within the pedicle, thereby securing the spinal segment. This
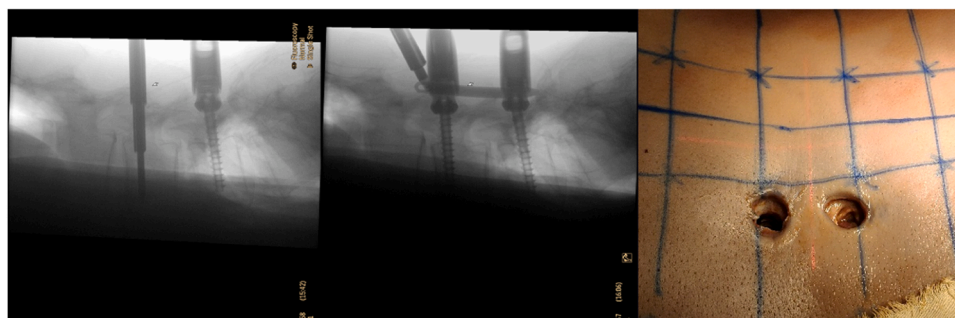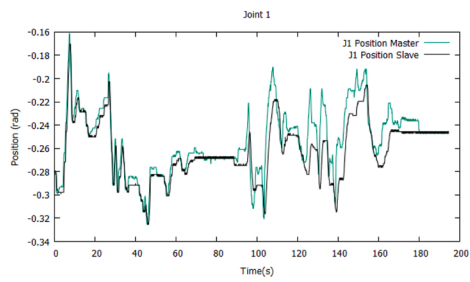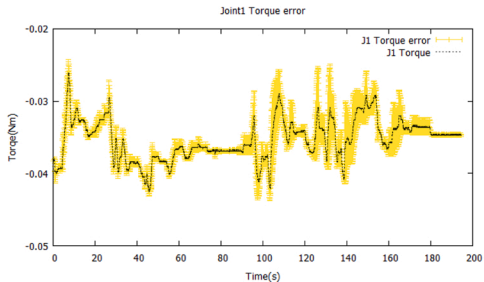

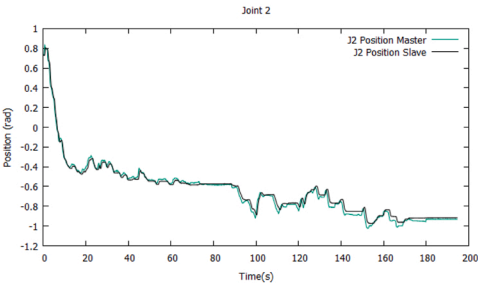**Fig. 9.** The successful of percutaneous robot-assisted pedicle screw insertion on the L4 and L5.
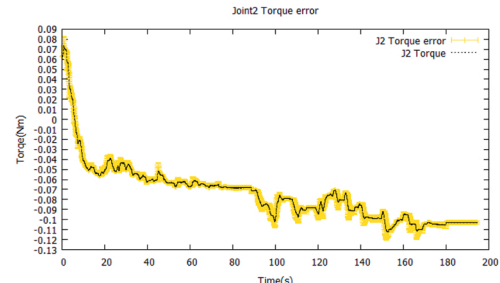
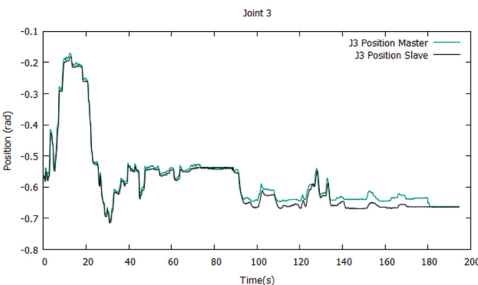(a) Master- Slave position response: Joint 1

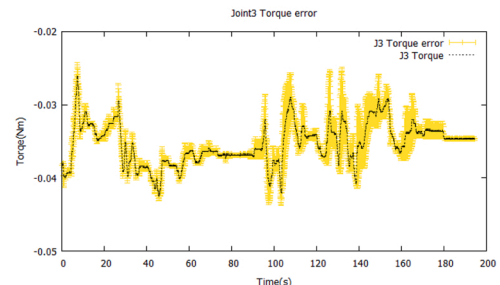(f) Torque response and error: Joint 1

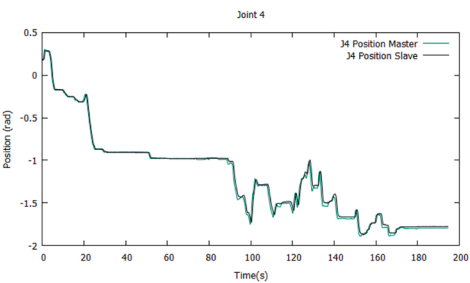(b) Master- Slave position response: Joint 2

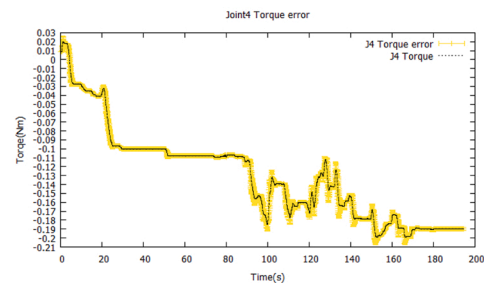(g) Torque response and error: Joint 2

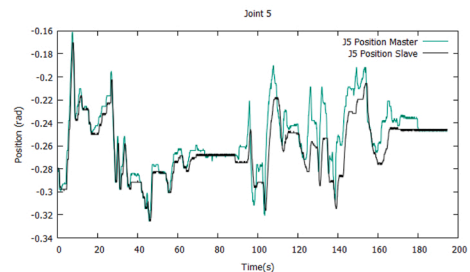(c) Master- Slave position response: Joint 3

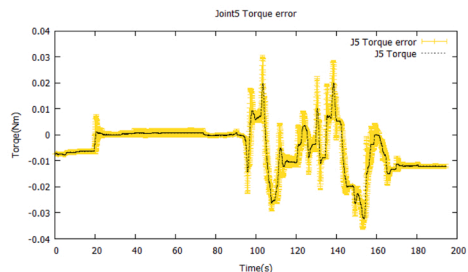(h) Torque response and error: Joint 3

(d) Master- Slave position response: Joint 4

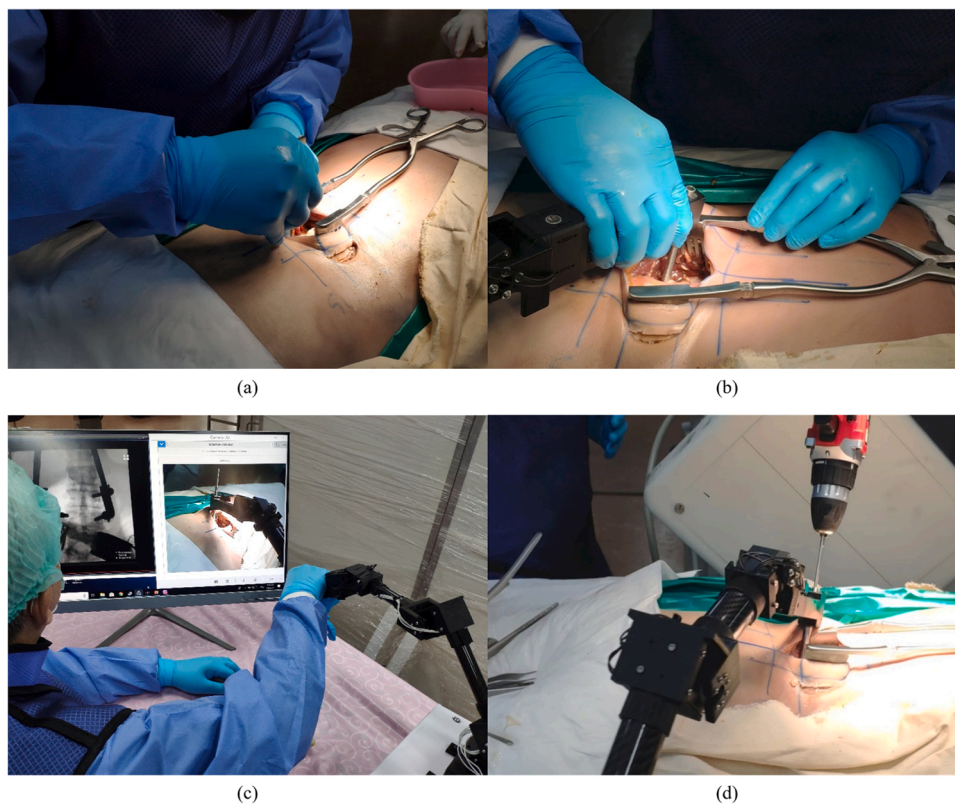(i) Torque response and error: Joint 4


(e) Master- Slave position response: Joint 5

(j) Torque response and error: Joint 5

Fig. 10. Robot-assisted pedicle screw Insertion (a-e) The position response of master-slave manipulator. (f-j) The torque response error of the master-slave manipulator.

Fig. 11. The open pedicle screw insertion with robot-assisted experiment (a). The surgeon performs a midline skin incision (b). The slave manipulator is moved to the entry point of pedicle (c). The surgeon remotely controls the slave manipulator via a master manipulator (d). The surgeon drills the pedicle through the guided sleeve.
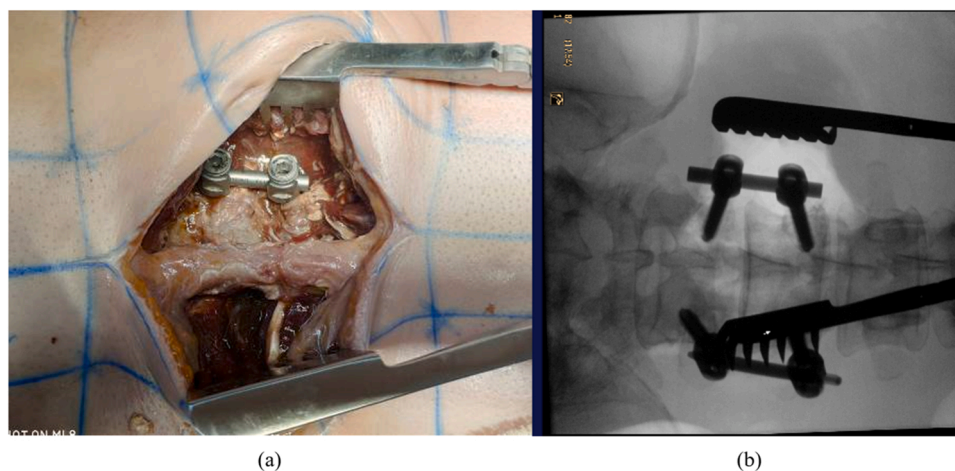

Fig. 12. The open pedicle screw insertion with robot-assisted experiment.

detailed documentation of the procedure not only illustrates the steps involved but also highlights the precision and safety enhancements afforded by the robotic assistance in spinal surgeries.

In the experimental analysis of the robot-assisted open pedicle screw insertion, the performance of the master-slave manipulator system was critically assessed through detailed measurements of position and torque responses. The results of this analysis are presented in Fig. 13, which is divided into parts **(a-e)** for position responses and parts **(f-j)** for torque error responses across the five joints of the manipulator. The position response of the master-slave manipulator, as detailed in Fig. 13(a-e), shows a high degree of fidelity between the master and the slave manipulators during the procedure. The graphs demonstrate that the joint

movements of the slave manipulator are well-aligned with those of the master manipulator, indicative of precise control and effective replication of intended movements. The mean position errors between the master and slave manipulators for each of the five joints were minimal, recorded as 0.01, 0.014, 0.018, 0.005, and 0.011 radians, respectively. These values signify an exceptional level of accuracy in the robotic system's ability to mirror the surgeon's movements, thus underscoring the system's reliability in surgical applications. Fig. 13(f-j) elaborates on the torque response errors between the master and slave manipulators. The error bars depicted in these segments of the figure indicate negligible discrepancies in the reaction torques across the joints, which are quantified as mean torque errors of 0.001, 0.0014, 0.0018, 0.0004, and
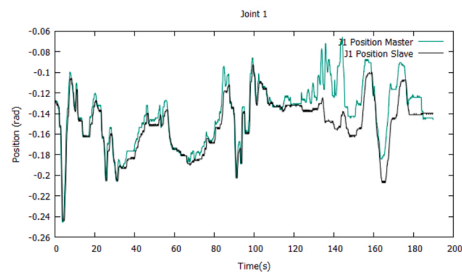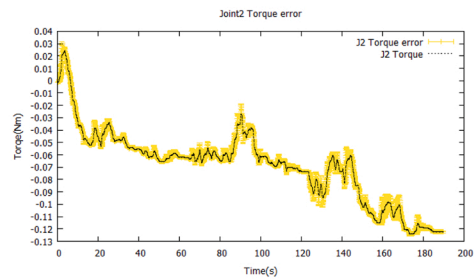
(a) Master- Slave position response: Joint 1
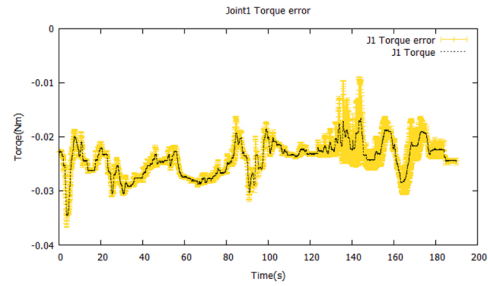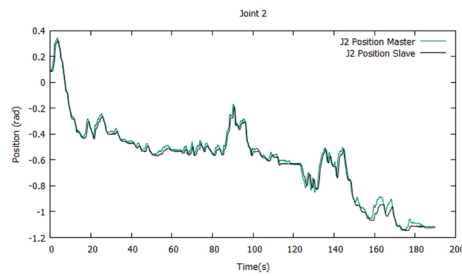
(f) Torque response and error: Joint 1

(b) Master- Slave position response: Joint 2

(g) Torque response and error: Joint 2

(c) Master- Slave position response: Joint 3

(h) Torque response and error: Joint 3

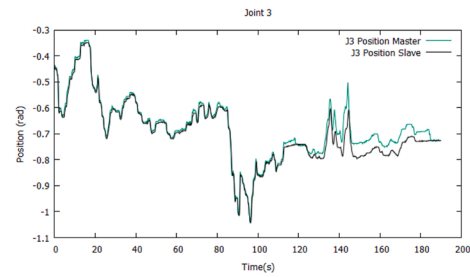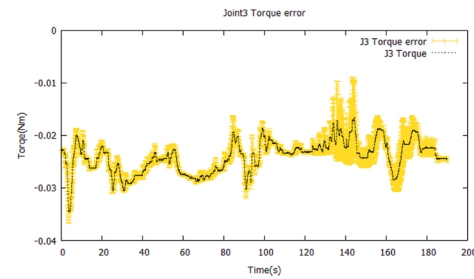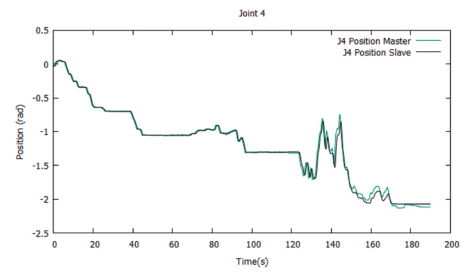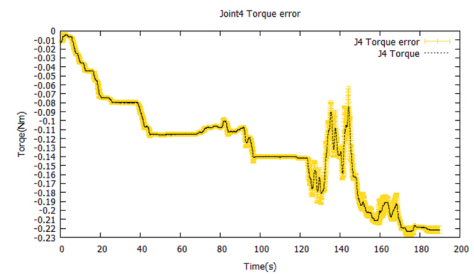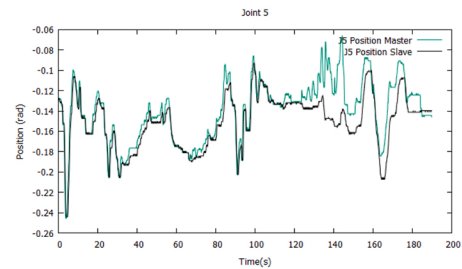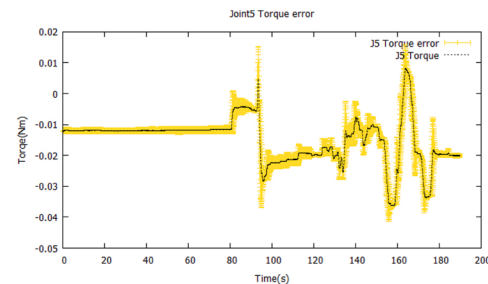(d) Master- Slave position response: Joint 4

(i) Torque response and error: Joint 4

(e) Master- Slave position response: Joint 5

(j) Torque response and error: Joint 5

Fig. 13. The open pedicle screw insertion with robot-assisted experiment. (a-e) The position response of master-slave manipulator, (f-j) The torque response error of the master-slave manipulator.

0.0011 Nm for each joint, respectively. These low error values highlight the system's precision in force feedback, which is crucial for maintaining the tactile feel necessary for sensitive surgical operations like pedicle screw insertion.

The combined data from the position and torque response analyses illustrate a robotic system that not only achieves a high degree of mechanical precision but also maintains a crucial tactile feedback loop between the surgeon and the procedure site. Such characteristics are vital for enhancing the safety, accuracy, and efficiency of spinal surgeries, enabling surgeons to perform complex maneuvers with increased confidence and reduced risk of errors. The detailed results from this study, captured in Fig. 13, validate the effectiveness of the master-slave robotic manipulator in a controlled experimental setup, promising significant implications for its future application in clinical settings. This experiment thus marks a substantial advancement in the integration of robotic assistance in surgical procedures, particularly in enhancing the execution and outcomes of spine surgeries.

4. Discussion

The introduction of sensorless haptic feedback in robot-assisted pedicle screw insertion represents a significant advancement in the field of spinal surgery. This study, focused on the application of this innovative technology in lumbar spine surgery, underscores its potential to enhance surgical precision and safety while addressing some of the inherent challenges associated with traditional pedicle screw fixation methods. One of the primary concerns in conventional pedicle screw fixation is the reliance on fluoroscopic guidance, which not only increases the risk of radiation exposure to both the patient and the surgical team but also demands high levels of surgeon skill and concentration. The sensorless haptic feedback system developed in this study aims to mitigate these issues by minimizing the need for continuous fluoroscopic imaging once the initial setup is completed. The system's ability to provide real-time feedback and detect anatomical landmarks accurately reduces the frequency of fluoroscopy use, thus potentially lowering radiation exposure significantly. This feature not only enhances the safety profile of the surgical procedure but also contributes to better outcomes by reducing the likelihood of complications associated with excessive radiation. This system enhances intuitive and efficient surgeries by dynamically stabilizing and guiding tools based on the surgeon's input and tactile feedback, instead of merely maintaining tools in a pre-set position. While the initial cadaveric study did not focus on reducing radiation exposure but rather on validating the integration and precision of the haptic mechanism, future iterations aim to decrease the need for fluoroscopy. Additionally, the current system requires manual operation by a scrubbed surgeon, but plans are underway to refine this, enabling more seamless control and maintaining sterility throughout the procedure.

The robotic system was meticulously compared with traditional methods such as freehand, fluoroscopy-assisted, and navigated pedicle screw insertion techniques. The findings revealed that the robotic system might offer substantial improvements in terms of accuracy and radiation safety. For instance, the average position and torque errors recorded during the insertion of pedicle screws were remarkably low, indicating a high level of precision provided by the robotic system. These errors 0.011 radian and 0.054 Nm for percutaneous screws, and 0.0116 radian and 0.0057 Nm for open screws demonstrate the system's capability to execute delicate surgical tasks with minimal deviation from the intended trajectory. The minimal radian and Newton meter discrepancies observed during the experiments suggest that the robotic system can achieve a precision that rivals or exceeds that of traditional methods. This precision is critical in spinal surgery, where slight misalignments can lead to severe postoperative complications such as chronic pain or neurological deficits. Therefore, the clinical relevance of these findings cannot be overstated, as they indicate a promising direction for enhancing surgical accuracy and patient safety in spine surgery.

In this study, a limitation recognized was that the insertion of only four pedicle screws in the preliminary study might not suffice to convincingly demonstrate the efficacy and safety of the sensorless haptic feedback system. The rationale behind this limited number of insertions was to initially evaluate the feasibility and potential of the technology in a controlled setting before expanding the scope of the experiment. While the results of this preliminary cadaveric study are promising, further research is needed to establish the broader clinical applicability of the sensorless haptic feedback system. Future studies should involve larger sample sizes and diverse anatomical sites to ensure the reliability and generalizability of the findings. Additionally, clinical trials involving human subjects are necessary to fully understand the impacts of this technology in real-world surgical settings. Such studies would help to refine the system further and potentially lead to widespread adoption in clinical practice. The successful implementation of sensorless haptic feedback in robot-assisted pedicle screw insertion for lumbar spine surgery could significantly revolutionize the field. By improving surgical precision and reducing radiation exposure, this technology has the potential to enhance patient outcomes and redefine standard surgical practices in spine surgery. As the technology matures and undergoes further clinical evaluation, it may soon become a new standard of care, offering a safer, more efficient alternative to traditional surgical techniques.

5. Conclusion

The integration of sensorless haptic feedback into robot-assisted pedicle screw insertion represents a significant advancement in spinal surgery technology, addressing challenges such as limited visibility of anatomical landmarks and high radiation exposure. By achieving accurate pedicle screw placement with minimal errors, this proposed system demonstrates potential in enhancing surgical precision while reducing radiation exposure for patients and surgical teams. Moreover, the ergonomic benefits offered contribute to improved surgical performance. Further studies involving larger sample sizes and clinical trials are necessary to establish the full clinical applicability and benefits of sensorless haptic feedback in spinal surgeries. Nevertheless, this research lays the groundwork for a safer, more precise, and less invasive approach to spinal surgery, promising improved patient outcomes and surgical practices in the future.

Ethical approval

Cadaveric based experiments were conducted, and the study was conducted in accordance with the Declaration of Helsinki and approved by the Institutional Review Board of the Mahidol University, SIRB Protocol No: 568/2563 for studies involving humans. Informed consent was obtained from the family members/ surrogate of all cadavers involved in the study.

Funding

CRediT authorship contribution statement

Sakol Nakdhamabhorn: Conceptualization, Data curation, Formal analysis, Methodology, Resources, Software, Validation, Visualization, Writing – original draft, Writing – review & editing. **Branesh M. Pillai:** Data curation, Formal analysis, Investigation, Methodology, Project administration, Resources, Software, Validation, Visualization, Writing – original draft, Writing – review & editing. **Areesak Chotivichit:** Conceptualization, Data curation, Formal analysis, Investigation, Methodology, Resources, Supervision, Validation, Visualization,

Writing – review & editing. **Branesh M Pillai:** Data curation, Formal analysis, Investigation, Methodology, Project administration, Resources, Software, Validation, Visualization, Writing – original draft, Writing – review & editing. **Jackrit Suthakorn:** Conceptualization, Data curation, Formal analysis, Funding acquisition, Investigation, Methodology, Project administration, Resources, Software, Supervision, Validation, Visualization, Writing – original draft, Writing – review & editing.

Declaration of Competing Interest

The authors declare that they have no known competing financial interests or personal relationships that could have appeared to influence the work reported in this paper.

Data availability

The data and analyses scripts used to support the findings of this study are available at https://datadryad.org/stash/share/ilhDAhX4U_hsBUmoyCjlZpCICWN2B2nP16oms8MiR1M.

Acknowledgments

References

[1] Kocis J, Kelbl M, Kocis T, Návrat T. Percutaneous versus open pedicle screw fixation for treatment of type A thoracolumbar fractures. Eur J Trauma Emerg Surg 2020;46:147–52.

[2] Tarawneh AM, Haleem S, D'Aquino D, Quraishi N. The comparative accuracy and safety of fluoroscopic and navigation-based techniques in cervical pedicle screw fixation: systematic review and meta-analysis. J Neurosurg: Spine 2021;35(2):194–201.

[3] Liu MY, Tsai TT, Lai PL, Hsieh MK, Chen LH, Tai CL. Biomechanical comparison of pedicle screw fixation strength in synthetic bones: Effects of screw shape, core/thread profile and cement augmentation. PLoS One 2020;15(2):e0229328.

[4] Fatima N, Massaad E, Hadzipasic M, Shankar GM, Shin JH. Safety and accuracy of robot-assisted placement of pedicle screws compared to conventional free-hand technique: a systematic review and meta-analysis. Spine J 2021;21(2):181–92.

[5] Naik A, Smith AD, Shaffer A, Krist DT, Moawad CM, MacInnis BR, Teal K, Hassaneen W, Arnold PM. Evaluating robotic pedicle screw placement against conventional modalities: a systematic review and network meta-analysis. Neurosurg Focus 2022;52(1):E10.

[6] Kuo KL, Su YF, Wu CH, Tsai CY, Chang CH, Lin CL, Tsai TH. Assessing the intraoperative accuracy of pedicle screw placement by using a bone-mounted miniature robot system through secondary registration. PloS One 2016;11(4):e0153235.

[7] Feng S, Tian W, Wei Y. Clinical effects of oblique lateral interbody fusion by conventional open versus percutaneous robot-assisted minimally invasive pedicle screw placement in elderly patients. Orthop Surg 2020;12(1):86–93.

[8] Peh S, Chatterjea A, Pfarr J, Schäfer JP, Weuster M, Klüter T, Seekamp A, Lipross S. Accuracy of augmented reality surgical navigation for minimally invasive pedicle screw insertion in the thoracic and lumbar spine with a new tracking device. Spine J 2020;20(4):629–37.

[9] Huntsman KT, Ahrendtsen LA, Riggleman JR, Ledonio CG. Robotic-assisted navigated minimally invasive pedicle screw placement in the first 100 cases at a single institution. J Robot Surg 2020;14(1):199–203.

[10] El-Desouky A, Silva PS, Ferreira A, Wibawa GA, Vaz R, Pereira P. How accurate is fluoroscopy-guided percutaneous pedicle screw placement in minimally invasive TLIF? Clin Neurol Neurosurg 2021;205:106623.

[11] Charles YP, Cazzato RL, Nachabe R, Chatterjea A, Steib JP, Gangi A. Minimally Invasive transforaminal lumbar interbody fusion using augmented reality surgical navigation for percutaneous pedicle screw placement. Clin Spine Surg 2021;34(7):E415–24.

[12] Wu C, Deng J, Li T, Tan L, Yuan D. Percutaneous pedicle screw placement aided by a new drill guide template combined with fluoroscopy: an accuracy study. Orthop Surg 2020;12(2):471–9.

[13] Han Z, Yu K, Hu L, Li W, Yang H, Gan M, Guo N, Yang B, Liu H, Wang Y. A targeting method for robot-assisted percutaneous needle placement under fluoroscopy guidance. Comput Assist Surg 2019;24(sup1):44–52.

[14] Kam JK, Gan C, Dimou S, Awad M, Kavar B, Nair G, Morokoff A. Learning curve for robot-assisted percutaneous pedicle screw placement in thoracolumbar surgery. Asian Spine J 2019;13(6):920.

[15] Nakdhamabhorn S, Suthakorn J. System integration of a fluoroscopic image calibration using robot assisted surgical guidance for distal locking process in closed intramedullary nailing of femur. Int J Electr Comput Eng 2019;9(5):3739.

[16] Chen HY, Xiao XY, Chen CW, Chou HK, Sung CY, Lin FH, Chen PQ, Wong TH. Results of using robotic-assisted navigational system in pedicle screw placement. PLoS One 2019;14(8):e0220851.

[17] Matsuoka A, Toyone T, Okano I, Kudo Y, Ishikawa K, Maruyama H, Ozawa T, Shirahata T, Inagaki K. Comparison of pedicle screw placement accuracy between two types of imaging support (Artis Zeego versus two-dimensional fluoroscopy): a cross-sectional observational study. BMC Musculoskelet Disord 2022;23(1):1–8.

[18] Kouyoumdjïan P, Gras-Combe G, Grelat M, Fuentes S, Blondel B, Tropiano P, Zairi F, Beaurain J, Charles YP, Dhenin A, Elfertit H. Surgeon's and patient's radiation exposure during percutaneous thoraco-lumbar pedicle screw fixation: A prospective multicenter study of 100 cases. Orthop Trauma: Surg Res 2018;104(5):597–602.

[19] Valentin J. The 2007 recommendations of the international commission on radiological protection. Oxford: Elsevier,; 2007.

[20] Stewart FA, Akleyev AV, Hauer-Jensen M, Hendry JH, Kleiman NJ, Macvittie TJ, Aleman BM, Edgar AB, Mabuchi K, Muirhead CR, Shore RE. ICRP publication 118: ICRP statement on tissue reactions and early and late effects of radiation in normal tissues and organs—threshold doses for tissue reactions in a radiation protection context. Ann ICRP 2012;41(1-2):1–322.

[21] European Society of Radiology (ESR) communications@ myESR. org. Summary of the European Directive 2013/59/Euratom: essentials for health professionals in radiology. Insights into Imaging 2015;6:411–7.

[22] Joseph JR, Smith BW, Liu X, Park P. Current applications of robotics in spine surgery: a systematic review of the literature. Neurosurg Focus 2017;42(5):E2.

[23] Dreval O, Rynkov I, Kasparova KA, Bruskin A, Aleksandrovskii V, Zil'Bernstein V. Results of using Spine Assist Mazor in surgical treatment of spine disorders. Interv (transpedicular Fixat) 2014;5(6)):9–22.

[24] Lieberman IH, Togawa D, Kayanja MM, Reinhardt MK, Friedlander A, Knoller N, Benzel EC. Bone-mounted miniature robotic guidance for pedicle screw and translaminar facet screw placement: Part I—Technical development and a test case result. Neurosurgery 2006;59(3):641–50.

[25] Togawa D, Kayanja MM, Reinhardt MK, Shoham M, Balter A, Friedlander A, Knoller N, Benzel EC, Lieberman IH. Bone-mounted miniature robotic guidance for pedicle screw and translaminar facet screw placement: part 2—evaluation of system accuracy. Neurosurgery 2007;60(2):129–39.

[26] Shoham M, Brink-Danan S, Friedlander A, Knoller N. Bone-mounted miniature robotic system for spine surgery. InThe First IEEE/RAS-EMBS Int Conf Biomed Robot Biomechatronics 2006:917–20. BioRob 2006. 2006.

[27] Tan LA, Lehman RA. Robotic-Assisted Spine Surgery Using the Mazor XTM System: 2-Dimensional Operative Video. Oper Neurosurg (Hagerstown, Md) 2019;16(4):E123.

[28] Mao G, Gigliotti MJ, Myers D, Yu A, Whiting D. Single-surgeon direct comparison of O-arm neuronavigation versus Mazor X robotic-guided posterior spinal instrumentation. World Neurosurg 2020;137:e278–85.

[29] Lefranc M, Peltier J. Accuracy of thoracolumbar transpedicular and vertebral body percutaneous screw placement: coupling the Rosa® Spine robot with intraoperative flat-panel CT guidance—a cadaver study. J Robot Surg 2015;9:331–8.

[30] Lefranc M, Peltier J. Evaluation of the ROSA™ Spine robot for minimally invasive surgical procedures. Expert Rev Med Devices 2016;13(10):899–906.

[31] Elswick CM, Strong MJ, Joseph JR, Saadeh Y, Oppenlander M, Park P. Robotic-assisted spinal surgery: current generation instrumentation and new applications. Neurosurg Clin 2020;31(1):103–10.

[32] Zygourakis CC, Ahmed AK, Kalb S, Zhu AM, Bydon A, Crawford NR, Theodore N. Technique: open lumbar decompression and fusion with the Excelsius GPS robot. Neurosurg Focus 2018;45(videosuppl1):V6.

[33] McDonnell JM, Ahern DP, Doinn TÓ, Gibbons D, Rodrigues KN, Birch N, Butler JS. Surgeon proficiency in robot-assisted spine surgery: a narrative review. Bone Jt J 2020;102(5):568–72.

[34] Pillai BM, Sivaraman D, Ongwattanakul S, Suthakorn J. Sensorless based gravity torque estimation and friction compensation for surgical robotic system. 2022 IEEE 9th Int Conf e-Learn Ind Electron (ICELIE) 2022:1–6.

[35] Nakdhamabhorn S, Pillai MB, Suthakorn J. Design and development of sensorless based 5-DOF bilaterally controlled surgical manipulator: A prototype. Bull Electr Eng Inform 2021;10(2):619–31.

[36] Madawala MK, Abeykoon AH, Mihiran BG, Mohottige DC, Meththananda RG, Pillai MB. Virtual torsional spring based bilateral control system for soft manipulation. In2013. Int Conf Circuits, Power Comput Technol (ICCPCT) 2013:337–43.

[37] Tian W, Han X, Liu B, Liu Y, Hu Y, Han X, Xu Y, Fan M, Jin H. A robot-assisted surgical system using a force-image control method for pedicle screw insertion. PloS One 2014;9(1):e86346.

[38] Boschetti G, Rosati G, Rossi A. A haptic system for robotic assisted spine surgery. Proc 2005 IEEE Conf Control Appl 2005:19–24. CCA 2005. 2005.

[39] Lauretti C, Cordella F, Tamantini C, Gentile C, di Luzio FS, Zollo L. A surgeon-robot shared control for ergonomic pedicle screw fixation. IEEE Robot Autom Lett 2020;5(2):2554–61.

[40] Wolf A, Shoham M, Michael S, Moshe R. Morphometric study of the human lumbar spine for operation–workspace specifications. Spine 2001;26(22):2472–7.

[41] Busscher I, Ploegmakers JJ, Verkerke GJ, Veldhuizen AG. Comparative anatomical dimensions of the complete human and porcine spine. Eur Spine J 2010;19:1104–14.

[42] Tondu B, Ippolito S, Guiochet J, Daidie A. A seven-degrees-of-freedom robot-arm driven by pneumatic artificial muscles for humanoid robots. Int J Robot Res 2005; 24(4):257–74.

[43] Pillai BM, Suthakorn J. Motion control applications: observer based DC motor parameters estimation for novices. Int J Power Electron Drive Syst 2019;10(1): 195–210.

[44] Furrer F, Burri M, Achtelik M, Siegwart R. Robot operating system (ros). Stud Comp Intell Vol 2016:625.

[45] Suthakorn J, Chirikjian GS. A new inverse kinematics algorithm for binary manipulators with many actuators. Adv Robot 2001;15(2):225–44.

[46] Diankov R. Automated construction of robotic manipulation programs (PhD dissertation). Carnegie Mellon University,; 2010.

[47] Pillai BM, Wilasrusmee C, Suthakorn J. Observer based dynamic control model for bilaterally controlled MU-lapa robot: Surgical tool force limiting. Int J Electr Comput Eng 2020;10(1):828.

[48] Ting HZ, Hairi M, Zaman M, Ibrahim M, Moubark A. Kinematic analysis for trajectory planning of open-source 4-DoF robot arm. Int J Adv Comput Sci Appl 2021;12(6):769–77.

[49] Faber H, Van Soest AJ, Kistemaker DA. Inverse dynamics of mechanical multibody systems: An improved algorithm that ensures consistency between kinematics and external forces. PloS One 2018;13(9):e0204575.

[50] Hasegawa Y, Kitamura T, Sakaino S, Tsuji T. Bilateral control of elbow and shoulder joints using functional electrical stimulation between humans and robots. IEEE Access 2020;8:15792–9.

[51] Jayasekara GM, Jayasingha PM, Jayalath PJ, Gomeda LH, Menikdiwela MP, Pillai MB, Abeykoon AH. Frequency response based analysis and designing of bilateral control system. 2014 Int Conf Circuits, Power Comput Technol [ICCPCT-2014] 2014:855–60.

[52] Harsha AM, Abeykoon S, Pillai MB. RTOS based embedded controller implementation of a bilateral control system. J Natl Sci Found Sri Lanka 2014;42 (3):217–28.

[53] Singh S, Choudhary NK, Lalin D, Verma VK. Bilateral ultrasound-guided erector spinae plane block for postoperative analgesia in lumbar spine surgery: a randomized control trial. J Neurosurg Anesthesiol 2020;32(4):330–4.

[54] Zhang H, Fang J, Yu H, Hu H, Yang Y. Disturbance observer-based adaptive position control for a cutterhead anti-torque system. Plos One 2022;17(5): e0268897.

[55] Pillai BM, Sivaraman D, Ongwattanakul S, Suthakorn J. Sensorless Based Gravity Torque Estimation and Friction Compensation for Surgical Robotic System. In2022. IEEE 9th Int Conf e-Learn Ind Electron (ICELIE) 2022:1–6.

[56] Ni J, Liu C, Liu H. Continuous uniformly finite time exact disturbance observer based control for fixed-time stabilization of nonlinear systems with mismatched disturbances. PloS One 2017;12(4):e0175645.

[57] Özbek NS. Design and real-time implementation of a robust fractional second-order sliding mode control for an electromechanical system comprising uncertainties and disturbances. Eng Sci Technol, Int J 2022;35:101212.

[58] Shikata K, Katsura S. Modal Space Control of Bilateral System with Elasticity for Stable Contact Motion. IEEJ J Ind Appl 2023;12(2):131–44.